H. Cost-Effective Machining of Titanium Materials

Albert J. Shih
Mechanical Engineering
University of Michigan
Ann Arbor, Michigan 48109-9379.
(734) 647-1766; fax: (734) 936-0363; e-mail: shiha@umich.edu

DOE Technology Development Area Specialist: Dr. Sidney Diamond
(202) 586-8032; fax: (202) 586-1600; e-mail: sid.diamond@ee.doe.gov
ORNL Technical Advisor: D. Ray Johnson
(865) 576-6832; fax: (865) 574-6098; e-mail: johnsondr@ornl.gov

---

Contractor: Oak Ridge National Laboratory, Oak Ridge, Tennessee
Prime Contract No: DE-AC05-00OR22725
Subcontractor: University of Michigan, Ann Arbor, Michigan

Objective

- Investigate new technologies for cost-effective machining of titanium (Ti) alloys.
- Gain in-depth knowledge of the effects of process parameters using three-dimensional (3D) finite element modeling (FEM).
- Study machining using a production tool with complicated geometry.
- Investigate tool wear mechanisms and investigate new tool materials and coatings.

Approach

- Experimentally validate force and temperature in 3D FEM.
- Conduct parametric study of the machining parameters using the validated model.
- Investigate the tool wear mechanisms and develop new tools and coatings.

Accomplishments

- Conducted turning and drilling experiments on Ti.
- Conducted 3D FEM of Ti turning and validated the cutting force and chip thickness with experimental measurements.
- Investigated the effects of cutting speed, a limiting factor for productivity in Ti machining.
- Conducted tool wear tests. Used the laser profilometry to study tool wear mechanism in Ti machining.

Future Direction

- Expand the drilling research to Ti drilling, an important and bottleneck process for engine manufacturing.
- Explore advanced tool materials and coatings for Ti machining.

Introduction

Titanium and its alloys are lightweight, corrosion-resistant, high-temperature materials. New emerging technologies have been developed to reduce the cost of producing raw Ti material and have brought the potential for low-cost Ti and for automotive applications.[1,2] While reducing the material cost can go a long way toward increasing the usage of Ti, high machining cost is another major technical barrier that needs to be overcome. To further reduce the cost of effective machining of Ti, a better understanding of the underlying mechanisms of the Ti machining process is necessary through better process and performance models, thermal modeling, and finite element simulation.[3] There is a lack of research in 3D FEM, which can provide detailed information about the stress, strain, and temperature distributions in the tool and workpiece; surface integrity of the part; and mechanics of chip curl. Advancements in machining process modeling have demonstrated the capability to provide reliable predictions of the performance of the cutting process and the influence of the process parameters on the product quality.[4]

Approach

Experimental Setup

The machining experiments were conducted on a Lodge and Shipley 30-hp computer numerically controlled lathe. A grade-two commercially pure (CP) Ti rod, 31.8 mm in diameter, was used. A left-handed tool holder, Kennametal CTAPL-163D, was used to hold the triangular-shaped insert. The tool holder controls the orientation of the tool and workpiece, which is defined by the lead, back rake, and side rake angles in turning.[5] The lead angle and back rake angle were 0°, the side rake angle was 5°, and the relief angle was 6°. A Kistler 9257A 3-axis piezoelectric dynamometer was used to measure cutting forces on the tool insert in three directions, which are designated as tangential force (F_t), radial force (F_r), and axial force (F_a), respectively. The force signal was processed using the charge amplifiers and recorded by a PC-based data-acquisition system.

FEM of 3D Turning of Titanium

The Third Wave Systems AdvantEdge™ 3D machining simulation software was used to model the Ti machining process. The updated-Lagrangian finite element method with continuous remeshing and adaptive meshing techniques was applied.[6] The coupling of the thermal and mechanical modeling of the tool and workpiece deformation was applied.[7] Figure 1 shows the initial 3D finite element mesh using a tool with a corner radius. An XYZ coordinate system is defined to show the relative orientation of the tool and cutting forces. The X-axis is the cutting direction. The Y-axis is the radial direction, which is parallel to the major cutting edge. The Z-axis is parallel to the axial direction of the rod workpiece. The 4-node, 12-degree-of-freedom tetrahedral finite element was used to model the workpiece and tool. The whole model includes approximately 100,000 nodes. The top and back surfaces of the tool are fixed in all directions. The workpiece is constrained in vertical (Z) and lateral (Y) directions on the bottom surface and moves at the cutting speed in the horizontal direction (–X) toward the stationary tool.

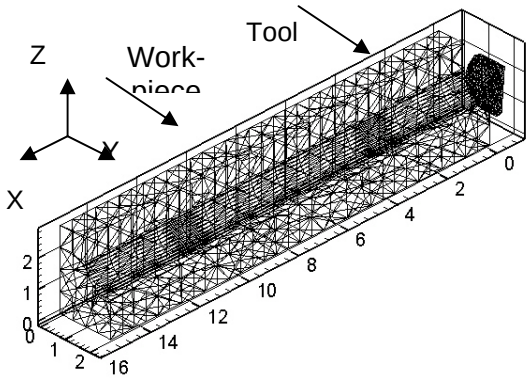

Figure 1. Initial finite element mesh for 3D turning model (unit: mm).

To validate the FEM, a baseline cutting test with four cutting speeds (24.4, 48.8, 97.5, and 195 m/min) and two feeds (0.254 and 0.381 mm/rev) was conducted at 1.02 mm depth of cut. Cutting forces were measured and compared with 3D finite element simulation results. One additional experiment was performed at a small depth of cut (0.254 mm) with a 48.8 m/min cutting speed and 0.254 mm/rev feed. All cutting tests were conducted dry without using cool-

ant. Nine simulations were conducted with the process parameters matched to those of the cutting experiments. The initial temperature was 20ºC.

Tool Wear Test

In the tool wear test, a tool insert was used to cut the Ti for an extended period of time to investigate the wear mechanism. Table 1 lists the corner radius and coating used in tool inserts for the wear test.

Table 1. Inserts and feed used for tool wear test (195 m/min cutting speed and 1.02 mm depth of cut)

Type[a]	TPG322	TPG320
Corner radius (mm)	0.8	0.1
Coating	No coating TiB_2	TiAlN TiB_2
Feed (mm/rev)	0.254	0.0508

[a]Kennametal tool number

The tool with a small, 0.1-mm corner radius was tested with a 0.254 mm/rev feed. The tip fractured prematurely. A smaller feed (0.0508 mm/rev) was therefore used for the tools with a 0.1-mm corner radius.

The flank wear was measured using an optical microscope. The width of flank wear land was recorded. The crater wear was measured using a laser profilometry (Rodenstock RM 600). The 3D surface topography of the tool rake face was recorded, and the volume loss on the tool rake surface was calculated.

Results

Experimental Validation of Cutting Forces

Figure 2 shows the comparison between the FEM (open symbol) and experimental measured (solid symbol) tangential, radial, and axial forces. For the tangential forces F_t, the finite element method generally underestimated by less than 15% with less discrepancy at high cutting speeds. For the radial and axial forces (F_r and F_a), the discrepancy was

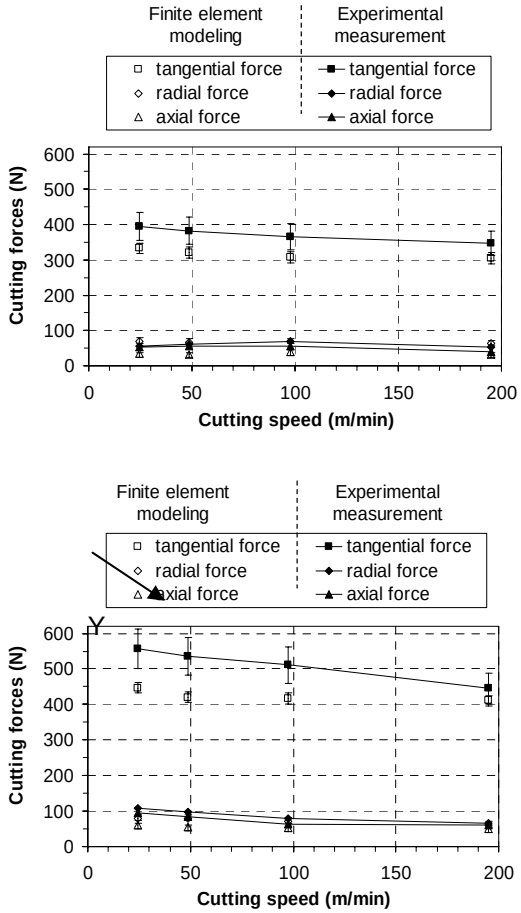

Figure 2. Comparison of cutting forces: (a) 0.254 and (b) 0.381 mm/rev feed.

less than 10% between the finite element simulation and experimental measurement results.

Although some discrepancies exist, the cutting force measurements validate the FEM results and set the direction for further refinement to improve the accuracy in modeling. The feed has a significant effect on the cutting force. At a high cutting speed, cutting forces were reduced slightly.

Cutting Speed Effects

Tool temperature is a key factor that accelerates tool wear and limits the cutting speed and productivity in Ti machining. Experimental measurement of tool temperature is difficult. However, a finite element simulation can provide a quick and accurate prediction of the tool temperature under various cutting conditions. The effect of cutting speed on tool temperature was investigated.

An example of the tool and workpiece temperature distributions of the nine 3D finite element cutting simulations is shown in Figure 3. The process parameters for the selected example are 195 m/min cutting speed, 0.254 mm/rev feed, 1.02 mm depth of cut, and 6.35 μm tool edge radius. The chip curl and the engagement of the tool and workpiece are shown in Figure 3(a). Figure 3(b) shows the tool temperature distribution. The high temperature is concentrated around the straight major cutting edge and the round corner of the tool. The peak temperature is about 480°C.

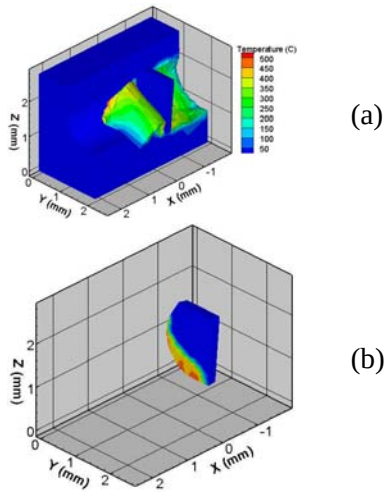

Figure 3. Temperature distributions: (a) workpiece and chip and (b) tool.

Figure 4 shows the peak temperature on the tool rake face of the eight baseline cutting experiments at two feeds and four cutting speeds.

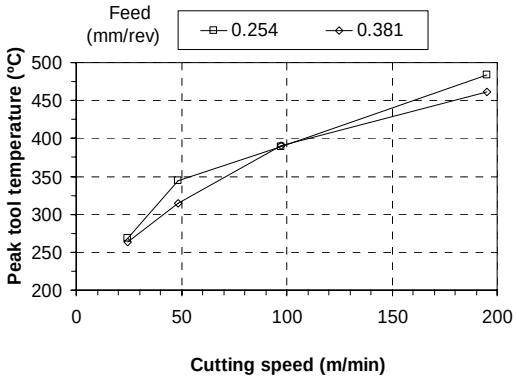

Figure 4. Peak tool temperature as a function of cutting speed.

The peak tool temperature is independent of the feed. This is comprehensible, since the very sharp tool cutting edge radius (6.35 μm) was used. The peak tool temperature increased significantly from about 260°C at a 24.4 m/min cutting speed to 480°C at 195 m/min. This demonstrates the effect of high-speed machining on tool temperature.

Chip Curl

This study explores the use of 3D FEM to predict the chip curl in turning. Figure 5(a) shows an experimental picture of the chip curl in machining of CP Ti with a 0.254-mm depth of cut, 48.8 m/min cutting speed, 0.254 mm/rev feed, and 0.8-mm tool corner radius. The change in cutting speed along the chip thickness is only 1.6%. The small change in cutting velocity across the chip thickness results in the up-curl dominated pattern. The effect of side-curl can also be seen to create the pitch of the curled chip. The tubular type helix chip is formed by rotational and translational motion along an axis parallel to the tool rake face.

The finite element method is applied to simulate cutting using the right-handed tool. Figure 5(b) shows a close-up view of a curled chip 15.2 mm in length in a 3D finite element simulation. Qualitatively, the morphology of the chip curl obtained from experimentation (Figure 5(a)) and FEM (Figure 5(b)) shows a similar pattern. The chip flow directions also match each other in FEM and experimental observation.

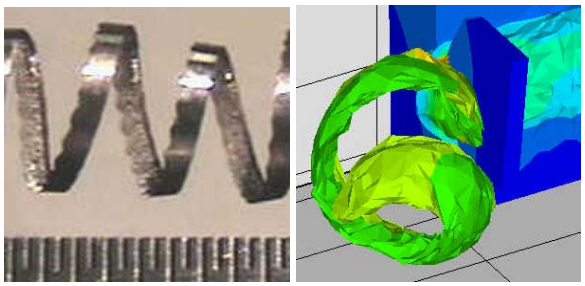

Figure 5. Chip curl with 0.254-mm depth of cut: (a) tubular chip in the experiment and (b) close-up view of the curled chip in simulation.

However, the finite element method underpredicts the radius and pitch of the chip curl by about 50%. One possible cause for this discrepancy is the contact of the chip with the tool, tool holder, and/or workpiece during cutting. Another possible cause is the external force acting on the chip from the weight of the chip after cutting. Since chip formation is con-

tinuous, the chip is pulled by its own weight to make a larger radius and pitch on the curled chip.

Tool Wear Test

Figure 6 shows the tangential forces (F_t) and the maximum width of flank wear land of the tool inserts.

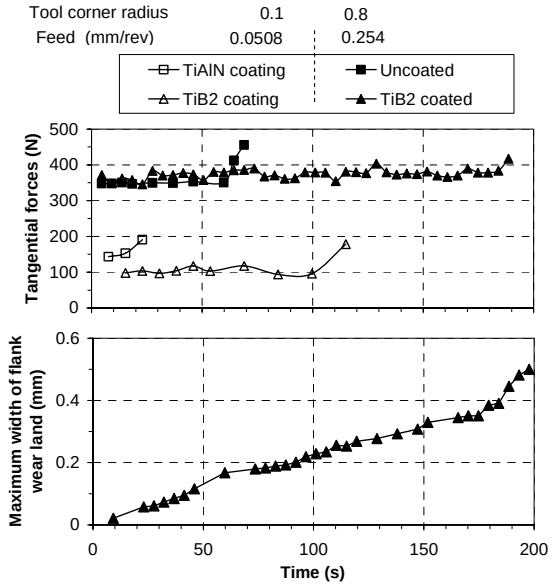

Figure 6. Tangential forces and the maximum width of flank wear land in Ti turning.

The tool life was determined at the time when the sharp increase in cutting forces occurred. For tools with a 0.8-mm corner radius, the life of uncoated and TiB_2-oated tools was 69 and 199 s, respectively. For tools with a 0.1-mm corner radius, the life of the TiAlN and TiB_2-coated tools was 15 and 115 s, respectively. TiAlN is a new type of coating, developed by Kennametal for interrupted cutting of Ti. It was not successful in the continuous turning of CP Ti. The flank wear of a TiB_2-coated tool with a 0.8-mm corner radius was measured by an optical microscope. A gradual increase in the maximum width of flank wear land can be seen in Figure 6. For the uncoated tool and tools with a 0.1-mm corner radius, because the tools were severely blurred with build-up material, no obvious flank wear could be observed.

Laser profilometry was applied to measure the crater wear. Figure 7 shows the SEM micrograph and the corresponding 3D laser profilometry measurement of the crater wear on the rake face of the TiB_2-coated tool with a 0.8-mm corner radius. The shape of crater wear can be observed. From the 3D contour shape of wear land, the volume of crater wear is calculated.

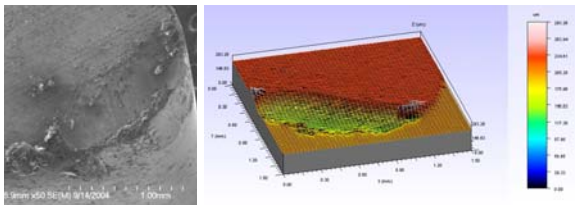

Figure 7. Crater wear of worn TiB_2-coated tool insert with 0.8-mm corner radius: (a) SEM micrograph and (b) 3D laser profilometry image.

Laser profilometry can also be used to quantitatively measure the shape of the build-up edge at the tool tip. Examples of the TiAlN and TiB_2-coated tool with a 0.1-mm corner radius are shown in Figure 8. The TiAlN obviously had a larger build-up edge, which resulted in the premature failure of the tool and the increase in the cutting force in Figure 6.

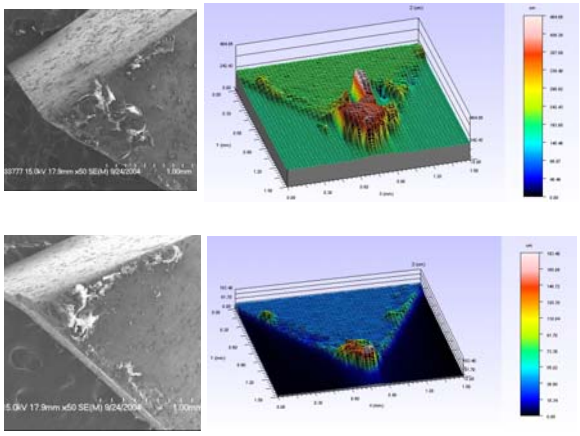

Figure 8. SEM micrograph and 3D laser profilometry image of the build-up edge at the tip of tool inserts with 0.1-mm corner radius: (a) TiAlN coated and (b) TiB_2 coated.

The friction coefficient of two types of tool coating was investigated. By dividing the cutting forces into the force components normal and parallel to the rake face, the coefficient of friction, μ, can be calculated by the following equations with 0° lead angle.

$$P = \sqrt{(F_t \sin\alpha + F_a \cos\alpha)^2 + F_r^2} \quad (1)$$

$$N = F_t \cos\alpha - F_a \sin\alpha \quad (2)$$

$$\mu = \frac{P}{N} \quad (3)$$

where

P is the force parallel to the rake face,
N is the force normal to the rake face,
α is the tool rake angle.

The coefficient of friction of a TiAlN-coated tool with a 0.1-mm corner radius was about 0.84, which was larger than the coefficient fractions of 0.52 and 0.34 of the TiB_2-coated tool with 0.1- and 0.8-mm corner radii, respectively.

Drilling

Drilling modeling is more complex than turning modeling. 3D drilling modeling is ongoing in close cooperation with Third Wave Systems. Figure 9 shows the preliminary result provided by Third Wave Systems. The chip was generated by drilling Al-6061 using a 9.35-mm-diameter WC-Co drill at 1.5 mm/rev feed and 40,000 rpm. The drill has a 30° helix angle, a 118° point angle, a 130° chisel edge angle, and a 2-mm web thickness. The modeling of Ti drilling is currently under development.

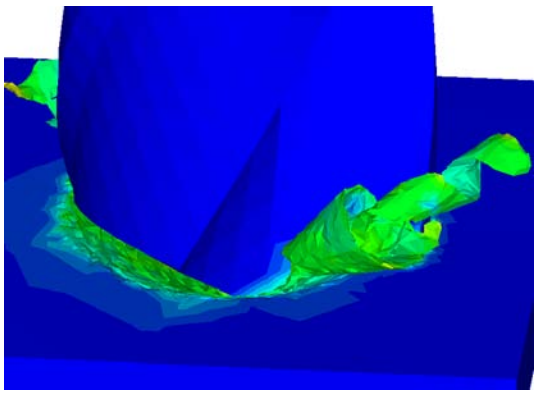

Figure 9. FEM of 3D drilling with chip generation.

Conclusions

The 3D finite element simulation of turning CP Ti was validated by comparing cutting forces with reasonable agreement. The effect of cutting speed on peak tool temperature was investigated. The application of finite element simulation to study the chip curl was explored. Qualitative agreement on the type of chip curl and chip flow direction were achieved for turning with a small depth of cut. The feasibility of using the finite element method to model the complicated 3D machining processes was demonstrated. The tool wear test demonstrated that a large tool corner radius and TiB_2 tool coating are more favorable to tool life than a small corner radius and TiAlN coating.

References

1. B. E. Hurless and F.H. Froes, "Lowering the Cost of Titanium," *The AMPTIAC Quarterly* **6**(2), 3–9 (2002).

2. E. H. Kraft, *Summary of Emerging Titanium Cost Reduction Technologies*, ORNL/Sub/4000023694/1, Oak Ridge National Laboratory, December 2003.

3. X. Yang, C. R. Liu, "Machining Titanium and Its Alloys," *Machining Science and Technology* **3**(1), 107–139 (1999).

4. K. F. Ehmann, S. G. Kapoor, R. E. Devor, I. Lazoglu, "Machining Process Modeling: A Review," *Journal of Manufacturing Science and Engineering* **119**, 655–663 (1997).

5. D. A. Stephenson and J. S. Agapiou, *Metal Cutting Theory and Practice*, Marcel Dekker, 1996.

6. T. D. Marusich, M. Ortiz, "Modeling and Simulation of High-Speed Machining," *International Journal for Numerical Methods in Engineering* **38**(21), 3675–3694 (1995).

7. A. J. Shih, "Finite Element Simulation of Orthogonal Metal Cutting," *ASME Journal of Engineering for Industry* **117**, 84–93 (1995).

Publications/Presentations

R. Li and A.J. Shih, "Finite Element Modeling of 3D Turning of Titanium," presented at the 2004 ASME IMECE, Anaheim, California, November 2004.

R. Li and A. J. Shih, "Finite Element Modeling of 3D Turning of Titanium," accepted for publication in *International Journal of Advanced Manufacturing Technology*.